

Lect. 7. CHGs and Optical Information Processing

7.1 Principles of optical information processing.

Optical information processing is based upon properties of lenses and parabolic mirrors to act in coherent radiation as a “chirp”- spatial light modulator and Fourier transformers. These properties are illustrated in Figs. 1-3.

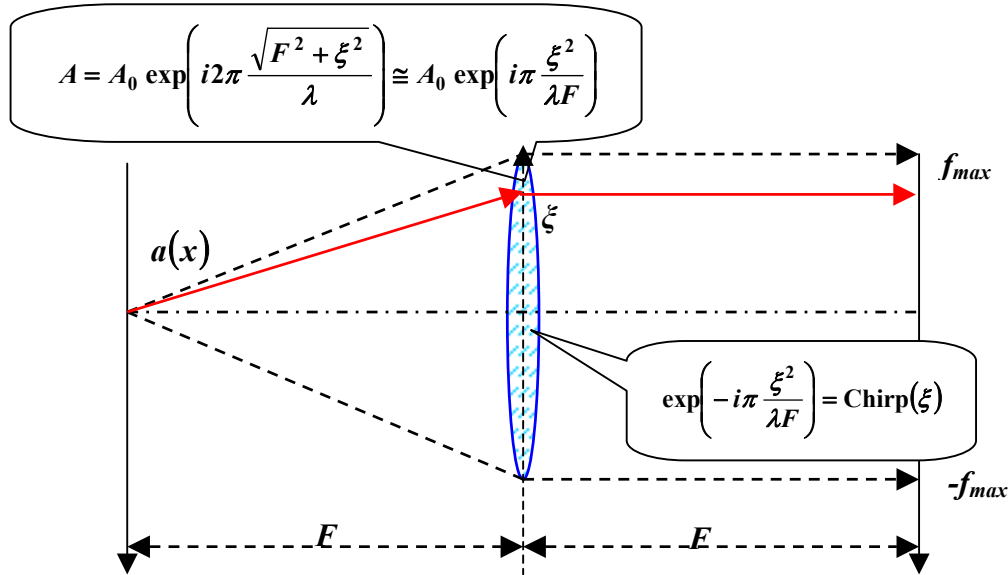


Fig. 7.1. Lens as a “chirp” spatial light modulator that converts spherical wave front to plane



Jean Baptiste Joseph Fourier (1768-1830)



Ernst Abbe, 1840-1905

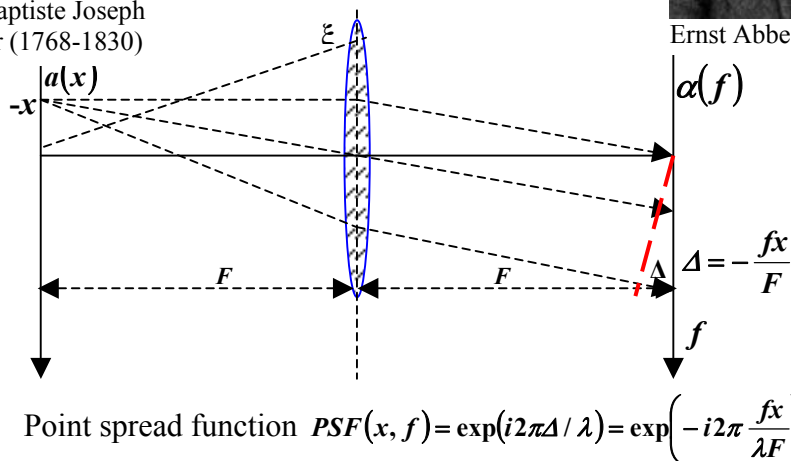


Fig. 7.2. Lens as Fourier processor that converts amplitude distribution of the wave front in its fore focal plane into distribution of its Fourier transform in the rear focal plane

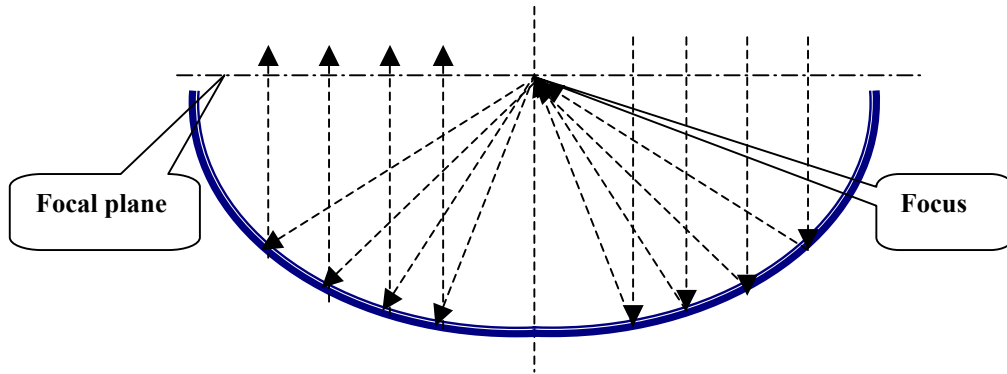


Fig. 7.3. Parabolic mirror as a “chirp” spatial light modulator and Fourier transformer

Schematic diagram of an optical information processing systems is shown in Fig. 7.4. Fig. 7.5 shows a schematic diagram of an optical information processing system in which lenses are replaced by a parabolic mirror as a Fourier processor. This replacement allows making the system to be more compact.

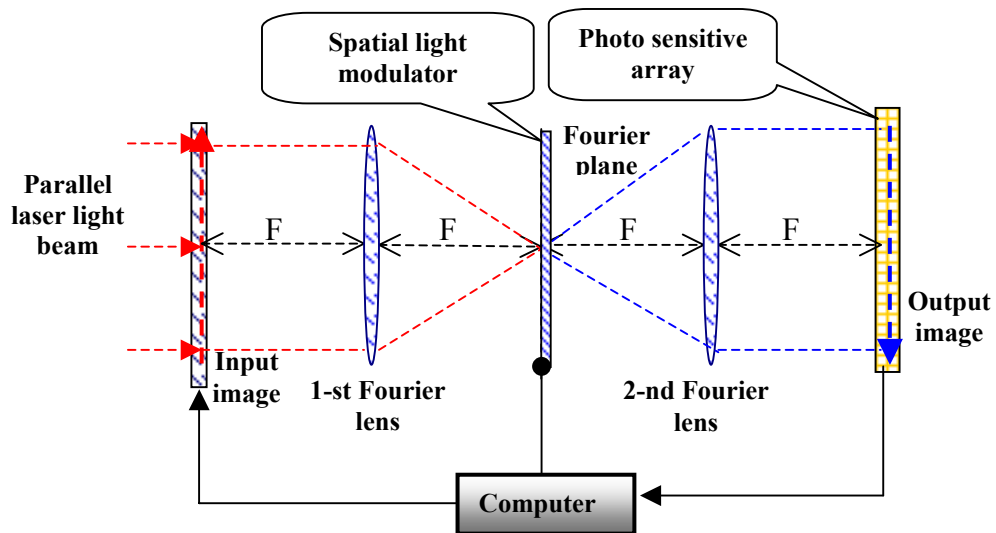


Fig. 7. 4-F electro-optical Fourier processor for image spatial filtering

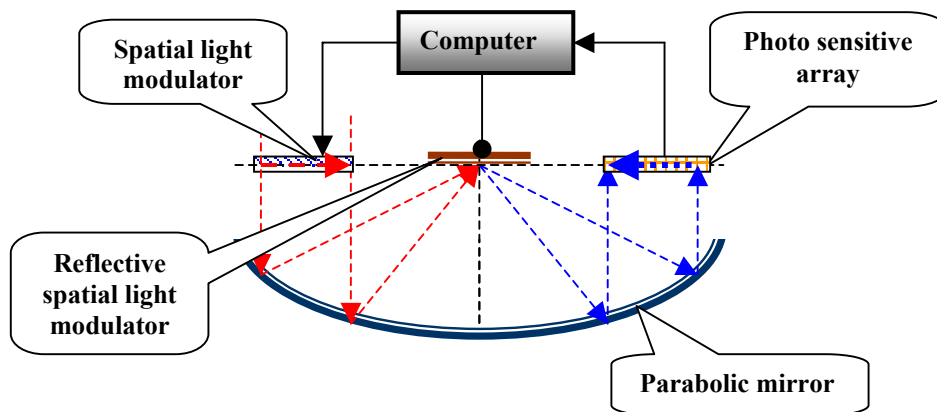


Fig. 7.5. Parabolic mirror electro-optical Fourier processor for image spatial filtering

7.2 Optimal adaptive correlator: theory

One of the most straightforward application of optical information processing systems is computing image correlation with a given template image. Optical correlators can be modeled as a device that consist of a linear filter followed by a device for locating the highest peak of the signal at the filter output as it is illustrated in the Figure 7.6.

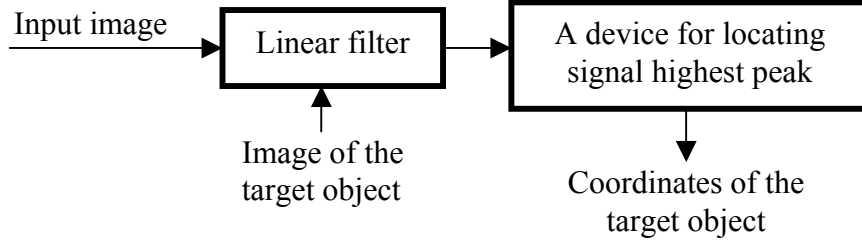


Fig. 7.6. Block diagram of a model of optical correlators for target detection and localization

The linear filter should be designed so as to minimize, on average over unknown target coordinates and image sensor's noise, the rate of false detections that occur in points, where signal at the filter exceeds the signal value at the point of the target location ([2,3]). Let b_0 be filter output signal value at the point (x_0, y_0) of target location and $p(b_{bg}/(x_0, y_0))$ be probability density of the filter output signal $b_{bg}(x, y)$ over the part of the image that does not contain the target object. Then the rate of false detections on average $AV_{Sens}AV_{TrgCoord}[\cdot]$ over unknown target coordinates (x_0, y_0) and the image sensor's noise can be computed as

$$P_{fd} = AV_{Sens}AV_{TrgCoord} \left[\int_{b_0}^{\infty} p(b_{bg}/(x_0, y_0)) db_{bg} \right] = \int_{AV_{Sens}(b_0)}^{\infty} AV_{Sens}AV_{TrgCoord} [p(b_{bg}/(x_0, y_0))] db_{bg} \quad (7.1)$$

This rate has to be minimized by the appropriate design of the linear filter.

For target signal $a(x - x_0, y - y_0)$ located at coordinates (x_0, y_0) , output of the filter with frequency response $H(f_x, f_y)$ at the point (x_0, y_0) of the target location can be computed as

$$b_0 = \int_{-\infty}^{\infty} \int_{-\infty}^{\infty} \alpha(f_x, f_y) H(f_x, f_y) df_x df_y, \quad (7.2)$$

where $\alpha(f_x, f_y)$ is Fourier spectrum of the target signal $a(x, y)$. In order to analytically design the filter that minimizes the rate of false alarms, one needs also a relationship between the filter frequency response and the probability density of the filter output signal given filter input signal. However, such a relationship does not exist. It is known only that, by virtue of the central limit theorem, linear filtering tends to normalize distribution function of output signal and that the explicit dependence of

$h(\mathbf{b}_{bg})$ on the filter frequency response $H(\mathbf{f}_x, \mathbf{f}_y)$ may only be written for the second moment m_2^2 of the histogram using Parseval's relation for the Fourier transform:

$$m_2^2 = \int_{-\infty}^{\infty} b_{bg}^2 h(b_{bg}/(x_0, y_0)) db_{bg} = \int_{-\infty}^{\infty} b_{bg}^2 (x, y/x_0, y_0) dx dy = \int_{-\infty}^{\infty} \int_{-\infty}^{\infty} |\beta_{bg}^{(0,0)}(\mathbf{f}_x, \mathbf{f}_y)|^2 |H(\mathbf{f}_x, \mathbf{f}_y)|^2 d\mathbf{f}_x d\mathbf{f}_y, \quad (7.3)$$

where $\beta_{bg}^{(0,0)}(\mathbf{f}_x, \mathbf{f}_y)$ is Fourier spectrum of this background part. Correspondingly, the second moment of the averaged probability distribution function $AV_{Sens} AV_{TrgCoord} [p(\mathbf{b}_{bg}/(x_0, y_0))]$ can be computed as

$$AV_{Sens} AV_{TrgCoord} [m_2^2] = \int_{-\infty}^{\infty} b_{bg}^2 AV_{Sens} AV_{TrgCoord} [h(b_{bg}/(x_0, y_0))] db_{bg} = AV_{Sens} AV_{TrgCoord} \left[\int_{-\infty}^{\infty} b_{bg}^2 (x, y/x_0, y_0) dx dy \right] = AV_{Sens} AV_{TrgCoord} \left[\int_{-\infty}^{\infty} \int_{-\infty}^{\infty} |\beta_{bg}^{(0,0)}(\mathbf{f}_x, \mathbf{f}_y)|^2 |H(\mathbf{f}_x, \mathbf{f}_y)|^2 d\mathbf{f}_x d\mathbf{f}_y \right]. \quad (7.4)$$

Therefore, for the optimization of the localization device filter we will rely upon the Tchebyshev's inequality

$$Probability(x \geq \bar{x} + b_0) \leq \sigma^2 / b_0^2. \quad (7.5)$$

that connects the probability that a random variable x exceeds some threshold b_0 and the variable's mean value \bar{x} and standard deviation σ .

Applying this relationship to Eq.(7.1), we obtain:

$$\bar{P}_a = \int_{b_0}^{\infty} AV_{Sens} AV_{TrgCoord} [p(\mathbf{b}_{bg})] db_{bg} \leq AV_{bg} \frac{AV_{Sens} AV_{TrgCoord} [m_2^2 - \bar{b}^2]}{(AV_{Sens} [\bar{b}_0 - \bar{b}])^2}, \quad (7.6)$$

where \bar{b} is mean value of the distribution function $p(\mathbf{b}_{bg})$. By virtue of the properties of the Fourier Transform, the mean value of the background component of the image, \bar{b} , is determined by the filter frequency response $H(\mathbf{0}, \mathbf{0})$ at the point $(\mathbf{f}_x = \mathbf{0}, \mathbf{f}_y = \mathbf{0})$. Its value defines a constant bias of the signal at the filter output which is irrelevant for the device that localizes the signal maximum. Therefore, one can choose $H(\mathbf{0}, \mathbf{0}) = \mathbf{0}$ and disregard \bar{b} in (7.6). Then we can conclude that, in order to minimize the rate \bar{P}_a of false detection errors, a filter should be found that maximizes the ratio of its response \bar{b}_0 to the target object to standard deviation $(m_2^2)^{1/2}$ of its response to the background image component

$$SCIR = \frac{\bar{b}_o}{(m_2^2)^{1/2}} = \frac{\int_{-\infty}^{\infty} \int_{-\infty}^{\infty} AV_{Sens} [\alpha(f_x, f_y)] H(f_x, f_y) df_x df_y}{\left(\int_{-\infty}^{\infty} \int_{-\infty}^{\infty} AV_{Sens} AV_{TrgCoord} \left[|\alpha_{bg}^{0,0}(f_x, f_y)|^2 \right] H(f_x, f_y)^2 df_x df_y \right)^{1/2}} \quad (7.7)$$

We will refer to this ratio as to *signal-to-clutter ratio (SCIR)*.

From the Schwarz's inequality it follows that

$$\begin{aligned} & \int_{-\infty}^{\infty} \int_{-\infty}^{\infty} \alpha(f_x, f_y) H(f_x, f_y) df_x df_y = \\ & \int_{-\infty}^{\infty} \int_{-\infty}^{\infty} \frac{AV_{Sens} [\alpha(f_x, f_y)]}{\left(AV_{TrgCoord} |\alpha_{bg}^{0,0}(f_x, f_y)|^2 \right)^{1/2}} H(f_x, f_y) df_x df_y \leq \\ & \left\{ \int_{-\infty}^{\infty} \int_{-\infty}^{\infty} \frac{|AV_{Sens} [\alpha(f_x, f_y)]|^2}{AV_{TrgCoord} \left[|\alpha_{bg}^{0,0}(f_x, f_y)|^2 \right]} df_x df_y \right\}^{1/2} \left\{ \int_{-\infty}^{\infty} \int_{-\infty}^{\infty} H(f_x, f_y)^2 \left(AV_{TrgCoord} \left[|\alpha_{bg}^{0,0}(f_x, f_y)|^2 \right] \right) df_x df_y \right\}^{1/2} \end{aligned} \quad (7.8)$$

with equality taking place when

$$H(f_x, f_y) = \frac{AV_{Sens} [\alpha^*(f_x, f_y)]}{AV_{TrgCoord} \left[|\alpha_{bg}^{0,0}(f_x, f_y)|^2 \right]} \quad (7.9)$$

where asterisk * denotes complex conjugation and $AV[\cdot]$ denotes $AV_{Sens} AV_{TrgCoord} [\cdot]$. Therefore signal-to-clutter ratio is

$$SCR \leq \left\{ \int_{-\infty}^{\infty} \int_{-\infty}^{\infty} \frac{|AV_{Sens} [\alpha(f_x, f_y)]|^2}{AV_{Sens} AV_{TrgCoord} \left[|\alpha_{bg}^{0,0}(f_x, f_y)|^2 \right]} df_x df_y \right\}^{1/2} \quad (7.10)$$

reaching its maximum for the optimal filter defined by the equation:

$$H_{opt}(f_x, f_y) = \frac{AV_{Sens} [\alpha^*(f_x, f_y)]}{AV_{Sens} AV_{TrgCoord} \left[|\alpha_{bg}^{0,0}(f_x, f_y)|^2 \right]}, \quad (7.11)$$

This filter will be optimal for the particular observed image. Because its frequency response depends on the image background component the filter is adaptive. We will call this filter “*optimal adaptive correlator*”.

To be implemented, optimal adaptive correlator needs knowledge of power spectrum of the background component of the image. However coordinates of the

target object are not known. Therefore one cannot separate the target object and the background in the observed image and can not exactly determine the background component power spectrum and implement the exact optimal adaptive correlator. Yet, one can attempt to approximate it by means of an appropriate estimation of the background component power spectrum from the observed image.

There might be different approaches to substantiating spectrum estimation methods using additive and implant models for the representation of target and background objects within images.

In the additive model, input image $b(x, y)$ is regarded as an additive mixture of the target object $a(x - x_0, y - y_0)$ and image background component $a_{bg}(x, y)$:

$$b(x, y) = a(x - x_0, y - y_0) + a_{bg}(x, y), \quad (7.12)$$

where (x_0, y_0) are unknown coordinates of the target object. Therefore power spectrum of the image background component averaged over the set of possible target locations may be estimated as

$$\begin{aligned} AV_{TrgCoord} \left[\left| \alpha_{bg}^{(0,0)}(f_x, f_y) \right|^2 \right] &= \left| \beta(f_x, f_y) \right|^2 + \left| \alpha(f_x, f_y) \right|^2 + \\ &\beta^*(f_x, f_y) \alpha(f_x, f_y) AV_{TrgCoord} \left[\exp[i2\pi(f_x x_0 + f_y y_0)] \right] + \\ &\beta(f_x, f_y) \alpha^*(f_x, f_y) AV_{TrgCoord} \left[\exp[-i2\pi(f_x x_0 + f_y y_0)] \right], \end{aligned} \quad (7.13)$$

Functions $AV_{TrgCoord} \left[\exp[i2\pi(f_x x_0 + f_y y_0)] \right]$ and $AV_{TrgCoord} \left[\exp[-i2\pi(f_x x_0 + f_y y_0)] \right]$ are Fourier transforms of the distribution density $d(x_0, y_0)$ of the target coordinates:

$$AV_{TrgCoord} \left[\exp[i2\pi(f_x x_0 + f_y y_0)] \right] = \iint_{x_0 y_0} d(x_0, y_0) \exp[\pm i2\pi(f_x x_0 + f_y y_0)] dx_0 dy_0 \quad (7.14)$$

In the assumption that the target object coordinates are uniformly distributed within the input image area, these functions are sharp peak functions with maximum at $f_x = f_y = 0$ and negligible values for all other frequencies. Therefore, for the additive model of the target object and image background component, averaged power spectrum of the background component may be estimated as:

$$AV_{TrgCoord} \left[\left| \alpha_{bg}^{(0,0)}(f_x, f_y) \right|^2 \right] \cong \left| \beta(f_x, f_y) \right|^2 + \left| \alpha(f_x, f_y) \right|^2; f_x, f_y \neq 0. \quad (7.15)$$

The implant model assumes that

$$a_{bg}(x, y) = b(x, y)w(x - x_0, y - y_0), \quad (7.16)$$

where $w(x - x_0, y - y_0)$ is a target object window function:

$$w(x, y) = \begin{cases} 0 & \text{within the target object} \\ 1, & \text{elsewhere} \end{cases} \quad (7.17)$$

In a similar way as it was done for the additive model and in the same assumption of uniform distribution of the coordinates over the image area, one can show that in this case power spectrum of the background image component averaged over all possible target coordinates may be estimated as

$$AV_{TrgCoor} \left[\left| \alpha_{bg}^{0,0}(f_x, f_y) \right|^2 \right] \cong \iint |W(p_x, p_y)|^2 |\beta(f_x - p_x, f_y - p_y)|^2 dp_x dp_y, \quad (7.18)$$

where $W(f_x, f_y)$ is Fourier transform of the window function $w(x, y)$. This method of estimating background component power spectrum resembles the conventional methods of signal spectral estimation that assume convolving power spectrum of the signal with a certain smoothing spectral window function $\bar{W}(p_x, p_y)$.

Both models imply that, as a zero order approximation, input image power spectrum may be used as an estimate of the background component power spectrum:

$$AV_{TrgCoor} \left[\left| \alpha_{bg}^{0,0}(f_x, f_y) \right|^2 \right] \cong |\beta(f_x, f_y)|^2. \quad (7.19)$$

This approximation is justified by the natural assumption that the target object size is substantially smaller than the size of the input image and that its contribution to the entire image power spectrum is small with respect to that of the background image component.

As for the averaging over image sensor's noise, one can show that, in the assumption of additive signal-independent zero mean noise, this averaging will result in adding to the above estimates (7.15), (7.18) and (7.19) variance σ_n^2 of the noise. The same averaging over the image sensor's noise required, according to Eq. 7.11, for the target spectrum does not change it under the above assumption of additive signal-independent zero mean noise. In this way we arrive at the following three modifications of optimal adaptive correlators:

$$H_{opt}(f_x, f_y) = \frac{\alpha^*(f_x, f_y)}{|\beta(f_x, f_y)|^2 + |\alpha(f_x, f_y)|^2 + \sigma_n^2} \quad (7.20)$$

$$H_{opt}(f_x, f_y) = \frac{\alpha^*(f_x, f_y)}{\iint_{-\infty-\infty}^{\infty-\infty} |W(p_x, p_y)|^2 |\beta(f_x - p_x, f_y - p_y)|^2 dp_x dp_y + \sigma_n^2} \quad (7.21)$$

$$H_{opt}(f_x, f_y) = \frac{\alpha^*(f_x, f_y)}{|\beta(f_x, f_y)|^2 + \sigma_n^2} \quad (7.22)$$

7.3 Variety of optical correlators and comparison

Since invention of the optical correlator-matched filter by Van der Lugt ([1]), a variety of optical correlators has been suggested and studied:

- Matched filter (MF) correlator

$$OUTPUT = FT\{FT(INPUT) \cdot (FT(REFobj))^*\}$$

- Joint Transform Correlator

$$OUTPUT = FT\{FT(INPUT + REFobj)^2\}$$

- Phase-only filter (POF) correlator ([4])

$$OUTPUT = FT\left\{FT(INPUT) \cdot \frac{(FT(REFobj))^*}{|FT(REFobj)|}\right\}$$

- Phase-only (PO) correlator

$$OUTPUT = FT\left\{\frac{FT(INPUT)}{|FT(INPUT)|} \cdot \frac{(FT(REFobj))^*}{|FT(REFobj)|}\right\}$$

- Optimal adaptive correlator (OAC)

$$OUTPUT = FT\left\{\frac{FT(INPUT) \cdot (FT(REFobj))^*}{|FT(INPUT)|^2}\right\} =$$

$$FT\left\{\frac{FT(INPUT)}{[|FT(INPUT)|^2]^{1/2}} \cdot \frac{(FT(REFobj))^*}{[|FT(REFobj)|^2]^{1/2}}\right\}$$

- $(-k)$ -th law nonlinear correlator

$$OUTPUT = FT\left\{\frac{FT(INPUT) \cdot (FT(REFobj))^*}{(|FT(INPUT)|^2)^k}\right\}$$

- Binarized versions: amplitude or phase components of the correlator filter or both are binarized

In these formulas $FT(\cdot)$ denotes Fourier Transform operator, $INPUT$, $OUTPUT$ and $REFobj$ denote input image, output image and reference object image, correspondingly.

Optical implementation of the optimal adaptive correlators requires using non-linear signal transformation in the Fourier plane of the correlators. One of the option is using a nonlinear media with $(-k)$ -th law nonlinearity placed in the Fourier plane of the correlator slightly out of focus in order to image spectrum smoothing before its non-linear transformation. Even more straightforward option is the non-linear Joint Transform Correlator with a logarithmic nonlinearity. Block diagrams of the nonlinear

optical correlator with k -th law nonlinearity and nonlinear Joint Transform correlators are shown in Figures 7.7 and 7.8. Note that these correlators can also be used as general image Fourier processors.

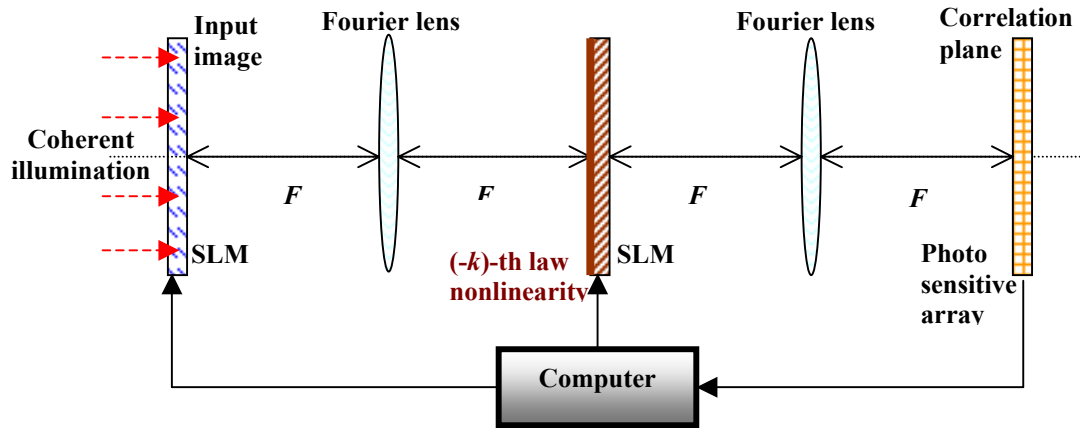


Fig. 7.7. $4-F$ nonlinear electro-optical correlator and Fourier processor. F – focal distance of the Fourier lens.

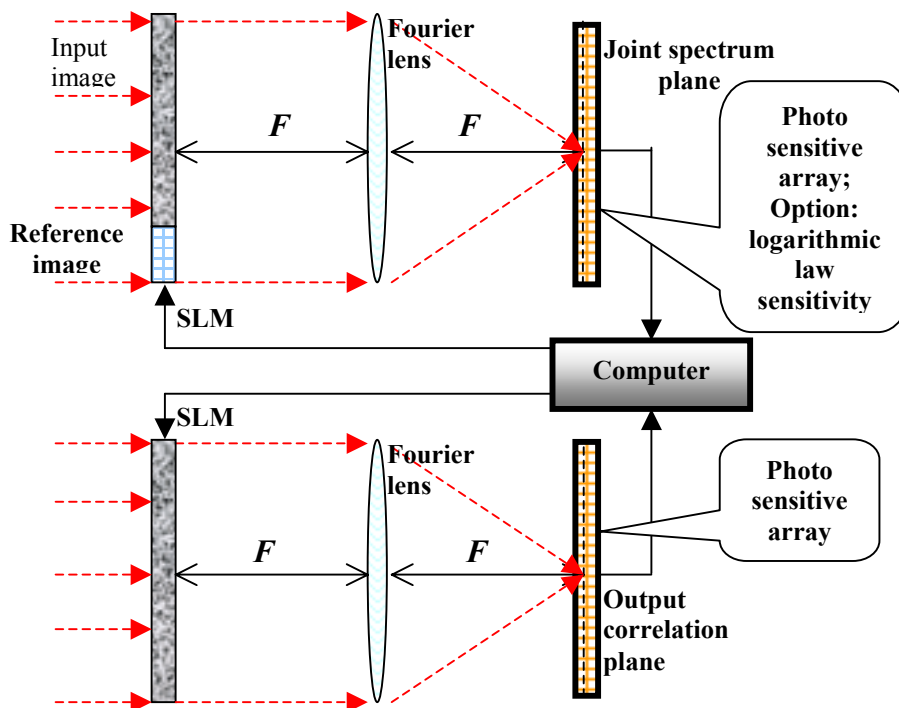


Fig. 7.8. Nonlinear Joint Transform optical modulator and Fourier processor. F – focal distance of the Fourier lens.

In Figures 7.9-7.12, results of experimental comparison of discrimination capability of different above described optical correlators are presented. The results were obtained by computer simulation.

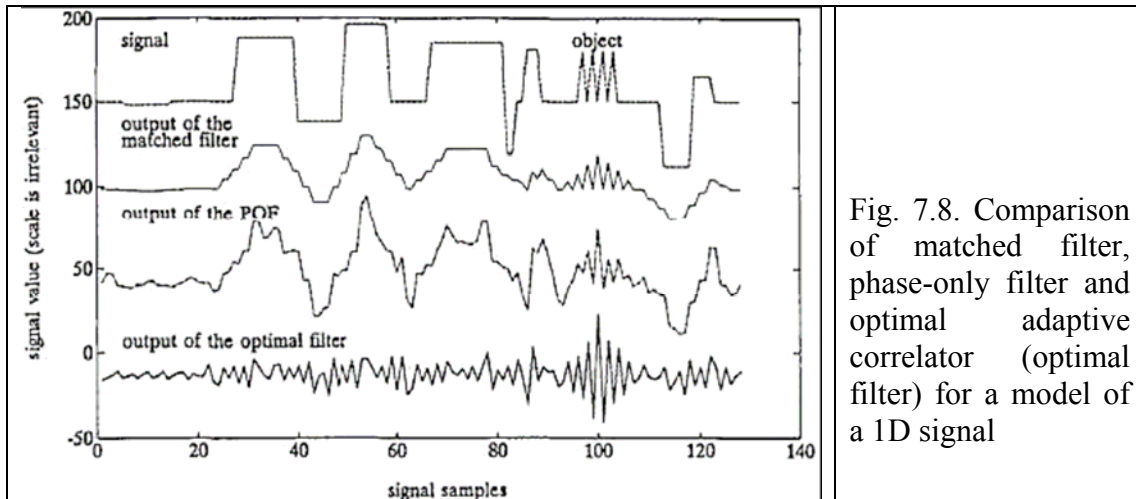


Fig. 7.8. Comparison of matched filter, phase-only filter and optimal adaptive correlator (optimal filter) for a model of a 1D signal

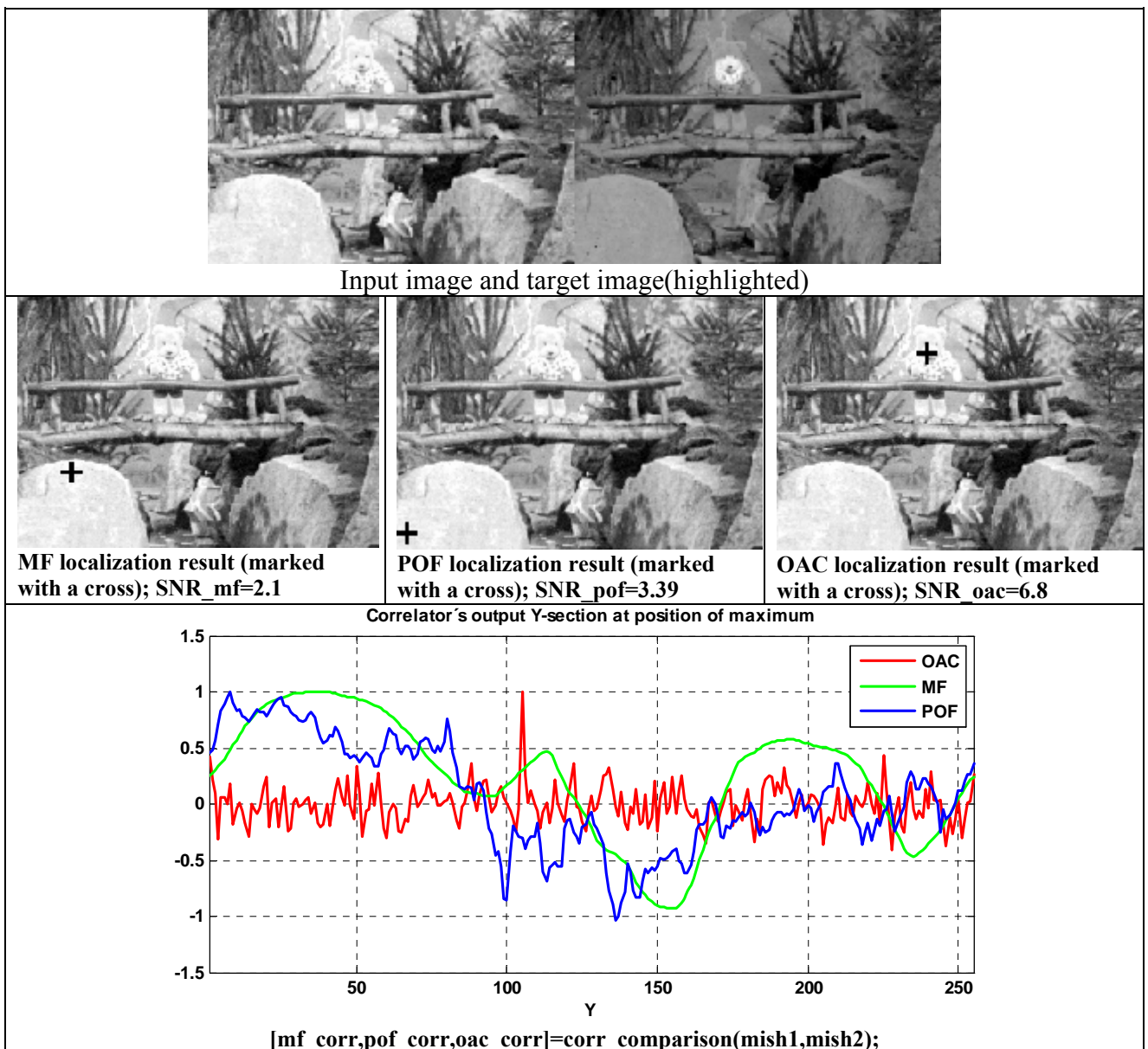


Fig. 7.10. Comparison of the matched filter, phase-only filter and optimal adaptive correlators for localization of corresponding points in stereoscopic images

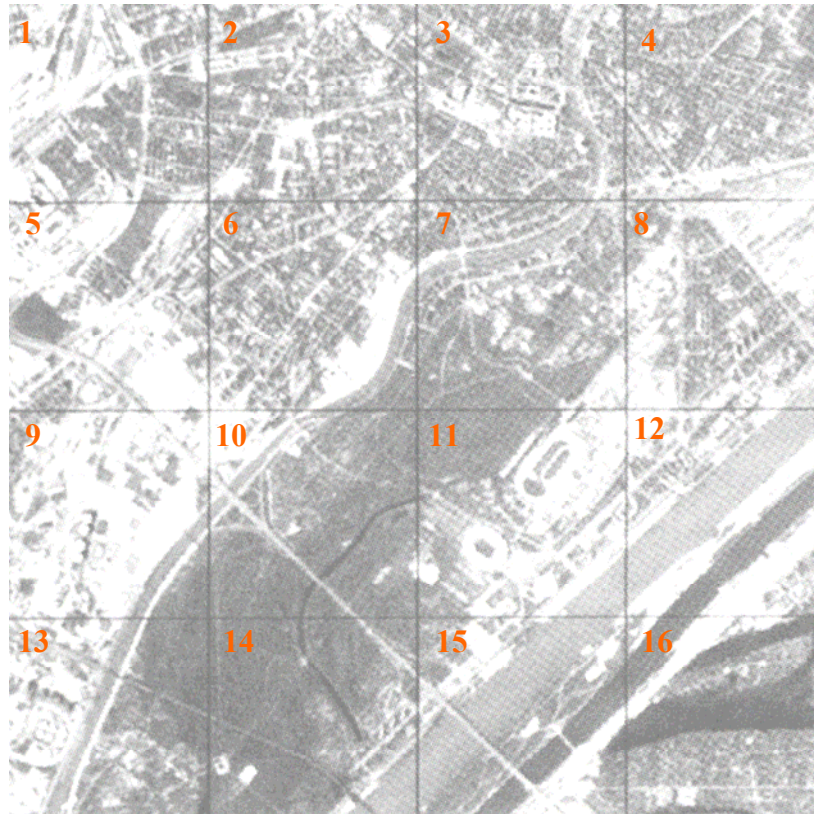


Fig. 7.10. Set of 16 test images of 128x128 pixels

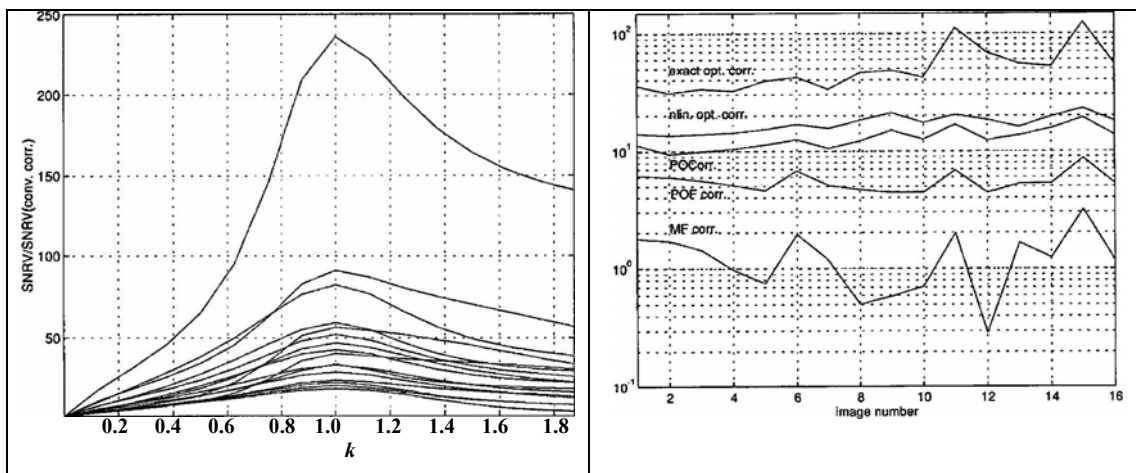


Fig. 7.10. Comparison, in terms of SCR, of the discrimination capability of the OAC (exact opt corr.), sub-optimal nonlinear optical correlators with the LS method of power spectrum estimation (nlin. opt. corr.), phase-only correlator (POCorr), phase-only filter (POF corr), and matched filter (MF corr) for the set of 16 test images and a circular target object of 5 pixels in diameter

7.4 Nonlinear Joint Transform Correlators

Consider frequency response (Eq. 7.20) of the optimal adaptive correlator obtained for the additive model of evaluating power spectrum of the background component of images and neglect in it variance of the additive sensor's noise:

$$H_{opt}(f_x, f_y) \cong \frac{\alpha^*(f_x, f_y)}{|\beta(f_x, f_y)|^2 + |\alpha(f_x, f_y)|^2}, \quad (7.24)$$

where $\beta(f_x, f_y)$ and $\alpha(f_x, f_y)$ are Fourier spectra of the image and target object, correspondingly, and let us now show that, with a logarithmic nonlinear transformation of the joint spectrum, the NLJTC approximates this filter. With the logarithmic nonlinearity, the transformed joint power spectrum $LogJPS(f_x, f_y)$ at the output of this nonlinear device can be written as

$$LogJPS(f_x, f_y) = \log \left\{ |\beta(f_x, f_y) + \alpha(f_x, f_y)|^2 \right\} = \log \left\{ |\beta(f_x, f_y)|^2 + |\alpha(f_x, f_y)|^2 + \beta^*(f_x, f_y)\alpha(f_x, f_y) + \beta(f_x, f_y)\alpha^*(f_x, f_y) \right\} \quad (7.25)$$

Since the size of the reference object is usually much smaller than the size of the input image, one can assume that, for the majority of the spectral components,

$$|\beta(f_x, f_y)|^2 + |\alpha(f_x, f_y)|^2 \gg \beta^*(f_x, f_y)\alpha(f_x, f_y) + \beta(f_x, f_y)\alpha^*(f_x, f_y) \quad (7.26)$$

With this assumption, $LogJPS(f_x, f_y)$ is approximately equal to

$$LogJPS(f_x, f_y) \cong \log \left\{ |\beta(f_x, f_y)|^2 + |\alpha(f_x, f_y)|^2 \right\} + \frac{\beta^*(f_x, f_y)\alpha(f_x, f_y)}{|\beta(f_x, f_y)|^2 + |\alpha(f_x, f_y)|^2} + \frac{\alpha^*(f_x, f_y)}{|\beta(f_x, f_y)|^2 + |\alpha(f_x, f_y)|^2} \beta^*(f_x, f_y) \quad (7.27)$$

When a JTC configuration is utilized, the two last terms displaying the correlation function and its conjugate are readily separated from each other and from the first term that produces the zero order diffraction term (see arrangement in Fig.). The last term of expression (7.27) exactly reproduces filtering described by Eq. 7.24. Therefore, one can conclude that the nonlinear joint transform correlator with the logarithmic non-linearity can be regarded as an approximation to the OAC and therefore promises an improved discrimination capability.

Logarithmic nonlinearity in JTC can be approximated by k -th law nonlinearity

$$Output = (Input)^k \quad (7.28)$$

for $k \ll 1$ provided appropriate normalization of the nonlinearity input signal to the fixed dynamic range. This is illustrated in Fig. 7.13.

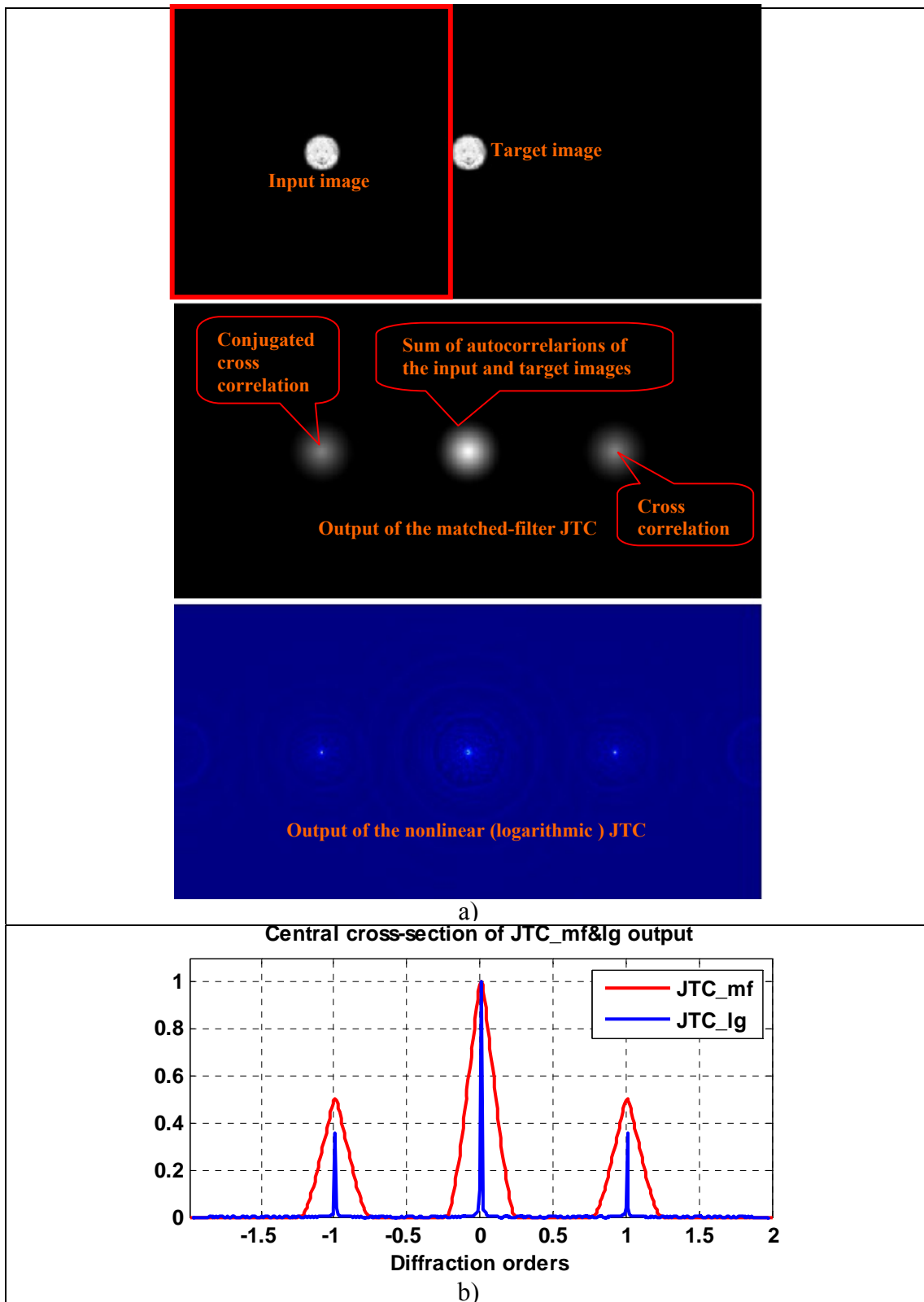


Fig. 7.12 a) Arrangement of input image and target object at the input of JTC and resulting correlation outputs of conventional linear (matched-filter) and nonlinear (logarithmic) JTCs; (b) Central cross sections of the matched-filter and nonlinear JTCs outputs for the test input image and target image shown in a).

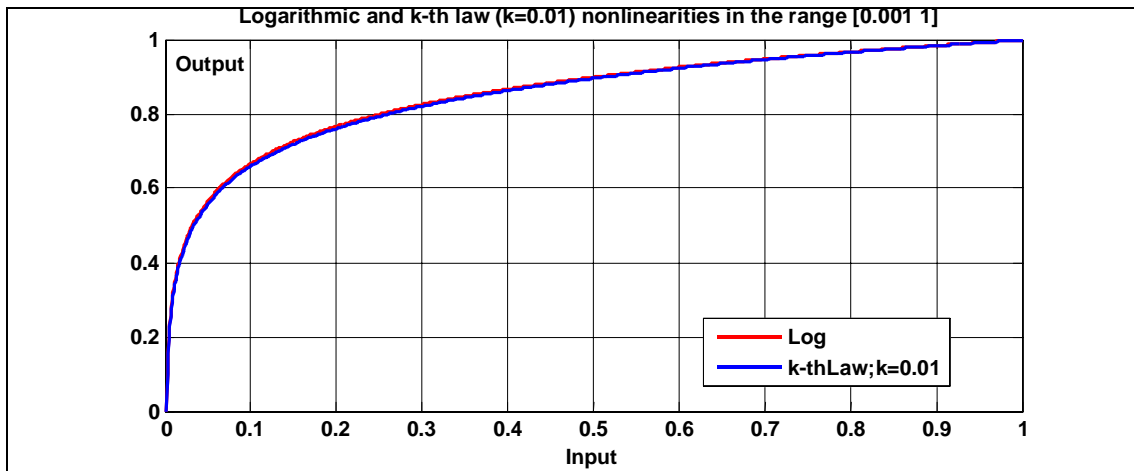


Fig. 7.13 Logarithmic and k -th law ($k=0.01$) nonlinearities in the dynamic range $[0.001 \div 1]$.

Experimental results, carried out with an account of the limited dynamic range of the nonlinearity in the nonlinear JTC correlators reported in [LPY Nonlinearity optimization] showed that

- Nonlinear JTC's with the k -th law nonlinearity ($k \ll 1$) may have a considerably improved discrimination capability in comparison with that of the JTC without non-linear transformation of the joint spectrum (case of $k = 1$). In terms of the Signal-to-Clutter Ratio, the observed gain, on average over the set of test images used in the experiments, exceeded 3 times. Comparison of the corresponding data for the nonlinear JTC's with the k -th law nonlinearity and the logarithmic JTC shows that, with an appropriate selection of the nonlinearity index k and the dynamic-range limitation threshold, the former performs slightly better.
- A trade-off exists between the nonlinearity index k and the dynamic-range limitation: a higher degree of dynamic-range limitation requires lower values of k . With this trade-off, the discrimination capability remains practically the same.
- The discrimination capability of the nonlinear JTC with the k -th law nonlinearity does not depend noticeably on k , provided that k exceeds a minimal value determined by the dynamic-range limitation level.

7.5 Color optical correlators

Color optical correlators can be implemented as separable component wise correlators with appropriate transformation of initial RGB-components ([7-9]). Block-diagram of such correlators is presented in Fig. 7.14. Computer simulation of such separable color correlators show that a considerable gain in correlator discrimination capability evaluated in terms of Signal-to-Clutter ratio can be obtained comparing to monochromatic images.

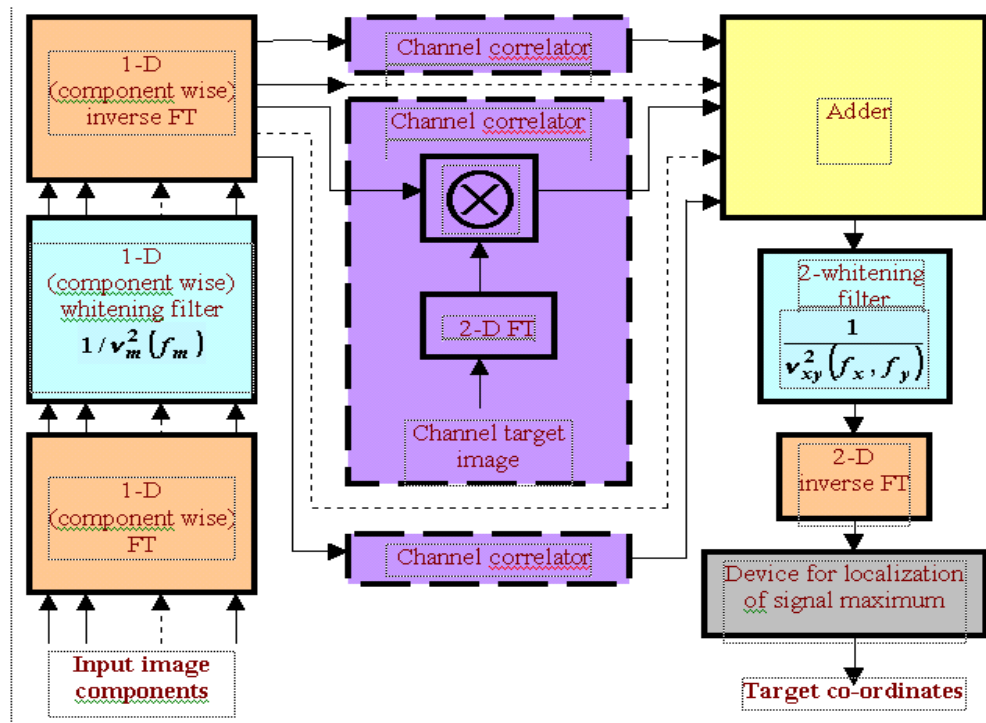


Fig. 7.14. Color 3-channel correlator with component conversion and spatial wise whitening

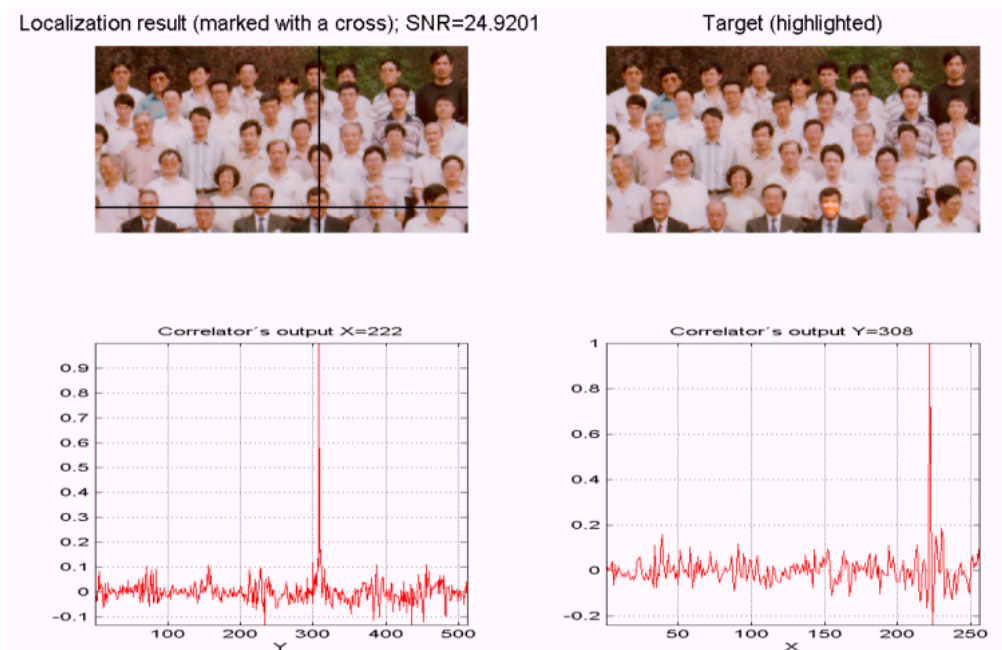


Fig. 7.14. Discrimination capability of the color correlator with component conversion

References

1. A. B. VanderLugt, "Signal detection by complex matched spatial filtering," *IEEE Trans. Inf. Theory* IT-10, 139-145 (1964).
2. L. P. Yaroslavsky, "The Theory of Optimal Methods for Localization of Objects in Pictures," *Progress in Optics Series*, Vol. 32 (Elsevier, Amsterdam, 1993), pp. 147-201.
3. L.P. Yaroslavsky, *Digital Holography and Digital Image Processing*, Kluwer Academic Publisher, Boston, 2004
4. J. L. Horner and P. D. Gianino, "Phase-only matched filtering," *Appl. Opt.* 23, 812-816 (1984).
5. L. P. Yaroslavsky, "Optical correlators with $(-k)$ -th law non-linearity: Optimal and suboptimal solutions," *Appl. Opt.* 34, 3924-3932 (1995).
6. L. Yaroslavsky, E. Marom, "Nonlinearity Optimization in Nonlinear Joint Transform Correlators," *Applied Optics*, vol. 36, No. 20, 4816-4822 (1997). (See also in: *Selected Papers on Optical Pattern Recognition Using Joint Transform Correlation*, M. S. Alam, ed., Milestone Series, v. MS 157, SPIE Optical Engineering Press, 1999)
7. V. Kober, V. Lashin, L. Moreno, J. Campos, L. Yaroslavsky, and M.J. Yzuel, "Color component transformations for optical pattern recognition," *JOSA, A*/vol. 14, No. 10/October 1997, pp.2656-2669.
8. I. Moreno, V. Kober, V. Lashin, J. Campos, L.P. Yaroslavsky, M. J. Yzuel, "Optical Color Pattern Recognition with Circular Component Decomposition," *Optics Letters*, V. 21, No. 7, April 1996, p. 498-500.
9. L. Yaroslavsky, "Optimal target location in color and multi component images," *Asian Journal of Physics*, Vol. 8, No 3 (1999) 355-369